ACS Energy LETTERS

http://pubs.acs.org/journal/aelccp

ENERGY EXPRESS

Fast Coevaporation of 1 μm Thick Perovskite Solar Cells

Manuel Piot, Javier Enrique Sebastian Alonso, Kassio P. S. Zanoni, Nathan Rodkey, Federico Ventosinos, Cristina Roldán-Carmona, Michele Sessolo,* and Henk Bolink*

Cite This: *ACS Energy Lett.* 2023, 8, 4711−4713

Read Online

ACCESS | Metrics & More | Article Recommendations | Supporting Information

ABSTRACT: **Coevaporation of perovskite films allows for a fine control over the material stoichiometry and thickness but is typically slow, leading to several-hour processes to obtain thick films required for photovoltaic applications. In this work, we demonstrate the coevaporation of perovskite layers using faster deposition rates, obtaining 1 μm thick films in approximately 50 min. We observed distinct structural properties and obtained devices with efficiency exceeding 19%, demonstrating the relevance of this deposition process from a material perspective and also in view of potential industrialization.**

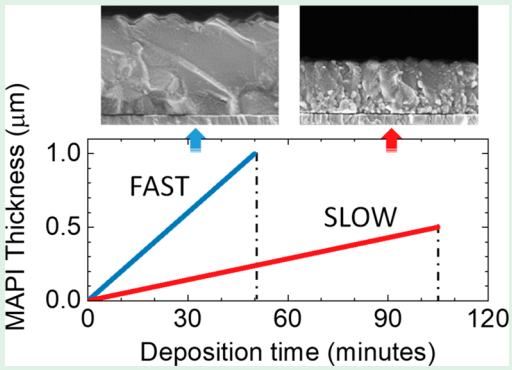

Vacuum deposition methods for perovskite film deposition are increasingly being adopted by the research community, as they allow for conformal deposition (important for perovskite/silicon tandem solar cells) and are more easily transferred to the industrial production environment.[1,2] Recently, several examples of vacuum-processed solar cells with power conversion efficiency (PCE) above 20% have been reported.[3−8] A benefit of vacuum deposition is the control over the perovskite thickness, which enables the use of micrometer thick films in photovoltaic devices. However, most coevaporations of hybrid perovskites are done at low overall deposition rate, resulting in long processes even for relatively thin (500 nm) films. This is because the control over of the deposition rate, *r*, of the organic precursors, such as methylammonium iodide (MAI), is not trivial. The adsorption on a substrate and hence *r*(MAI) are strongly dependent on the surface chemistry and temperature.[5,9,10] We have previously shown that the methylammonium lead iodide (MAPI) deposition can be accurately monitored using two quartz crystal microbalances (QCMs): one located above the PbI_2 thermal source to control $r(PbI_2)$, and the other at the level of the substrate (SBS), measuring *r*(SBS) as a sum of $r(PbI_2)$ and *r*(MAI). This process is very reproducible and is also independent of the purity of the MAI precursor.[11] In this work, we have increased the deposition rate to 4 times (x4) the standard rate (x1, the baseline from our previous work)[11] by increasing the temperature of the crucibles to achieve the desired rates (see Table S1 for the exact rates values). In Figure S1, the pressure, crucible temperature, and rates are presented for the x1 and x4 MAPI process, showing stable rates and temperature over the entire deposition process, irrespective of the overall deposition rate. Note that we have also explored higher deposition rates (up to x8), but in those cases we observed some fluctuations in the *r*(SBS), and also limitations in the QCM lifetime and amount of precursor due to the crucible volume. Figure 1 includes the characterization of MAPI films obtained using slow (MAPI x1, 680 nm thick) and fast (MAPI x4, 640 nm thick) deposition rates. The optical absorption (Figure 1a) cutoff is similar for the two perovskites, showing a bandgap of 1.60 eV (Tauc plot, Figure 1b). The slightly higher absorbance despite the thinner film for the MAPI x4 is a consequence of an increased absorption coefficient (Figure S3), suggesting that the material properties are dependent on the deposition rates. This is also supported by roughness measurements (Figure S4), which exclude a contribution from enhanced scattering. Note that the higher absorbance for the MAPI x4 at 800 nm is due to optical interference (Figure S5), a consequence of the different thickness and high optical quality of the films. The X-ray diffraction (XRD) patterns of the same perovskite films grown at different speeds are shown in Figure 1c. The

Received: August 18, 2023
Accepted: October 5, 2023

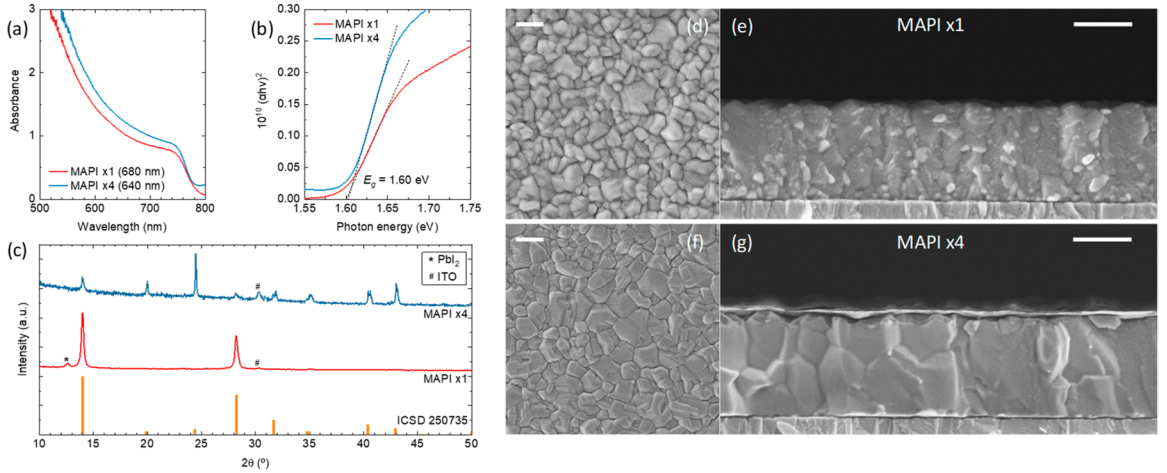

Figure 1. Characterization of MAPI films obtained at standard (x1) and fast (x4) deposition rates. (a) Optical absorption and (b) corresponding Tauc plot, (c) XRD analysis compared to a reference cubic pattern, and (d–g) SEM analysis (scale bar is 300 nm in all micrographs).

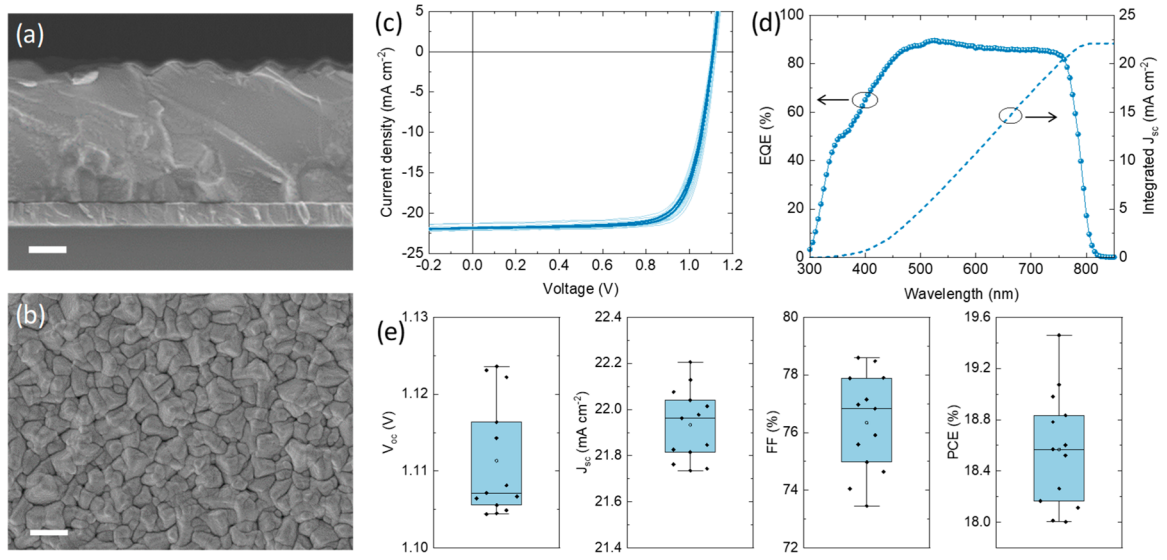

Figure 2. SEM micrograph of (a) the cross section and (b) surface of a 1 μm thick MAPI film deposited at 4 times the normal speed. (c) J–V curves under simulated solar illumination, (d) representative EQE spectrum, and (e) PV parameters.

MAPI x1 shows intense and single reflections at $2\theta = 14.2°$ and 28.5°, assigned to (001) and (002) planes of a cubic MAPI.[12] However, the crystal orientation differs when increasing the deposition rates, with a strongly suppressed intensity of the peak at $2\theta = 14.2°$ and a preferential growth along the (111) plane ($2\theta = 24.5°$) for MAPI x4. In addition, the signal-to-noise ratio is also lower for the MAPI x4 compared to the standard process, suggesting that the films have a lower degree of crystallinity.

The samples were further characterized by scanning electron microscopy (SEM). The standard MAPI x1 surface (Figure 1d) is composed of small grains (typical size in the 50–250 nm range) randomly arranged over the observation area. This surface morphology is a common feature of vacuum-deposited perovskite films, as highlighted in previous reports.[13] The film cross section (Figure 1e) shows a compact material with some small features that are randomly arranged through the layer. The surface morphology of MAPI x4 (Figure 1f) shows similar aggregates (in terms of size and distribution), although with a more compact morphology and faceted grains. More striking is the difference in the material cross section (Figure 1g), showing large and faceted grains arranged in a compact and void-free manner. Indeed, the SEM and XRD analyses confirm that the MAPI growth at higher deposition rate leads to different material properties, as already observed by the absorption spectra.

The film formed with the fast deposition protocol was tested in p-i-n solar cells employing the following stack: glass-ITO/CS90112 (2.5 nm)/TaTm (10 nm)/MAPI (1 μm)/C_{60} (10 nm)/BCP (7 nm)/Ag (100 nm)/Al_2O_3 (30 nm) (details are in the Supporting Information). Thanks to the faster deposition, 1 μm thick MAPI films can be deposited in only 50 min after stabilization of $r(PbI_2)$ and r(MAI). Although not optimized, this thickness would allow a quantitative light absorption even in the absence of a rear electrode, which is needed in tandem and bifacial devices. Figure 2a,b shows the SEM micrograph of the cross section and of the surface, confirming the monolithic and compact morphology observed before for thinner films. The current density vs voltage (J–V) curves under illumination for 12 solar cells produced in different deposition runs are shown in Figure 2c, together with their mathematical average. The J–V curves show small but appreciable hysteresis, which might be related with the increased roughness of the film (as inferred from

https://doi.org/10.1021/acsenergylett.3c01724
ACS Energy Lett. 2023, 8, 4711–4713

SEM and AFM). The short-circuit current density (J_{sc}) is approximately 22 mA/cm^2 for all samples. This is corroborated by the integration of the external quantum efficiency (EQE) over the AM1.5G solar irradiance spectrum. The EQE spectrum peaks at 90% at approximately 500 nm and is rather flat around 86% toward longer wavelengths. The corresponding PV parameters are reported in Figure 2e, with average open-circuit voltage (V_{oc}) of 1.1 V, fill factor (FF) of 77%, and PCE of 18.6%. The record pixels for these experiments reached a PCE of 19.4% in reverse bias scan (V_{oc} = 1.12 V; J_{sc} = 22.1 mA/cm^2; FF = 78.5%). This is close to the highest reported values for vacuum -deposited MAPI solar cells obtained at lower deposition rates,[3−5] indicating that fast processing is indeed compatible with efficient devices.

In conclusion, we present a fast process to deposit MAPI films by coevaporation. By using a two-QCM configuration, it is possible to control the process at increased deposition rates, allowing the fast deposition of 1 μm thick films. Importantly, MAPI films deposited at higher speeds show different morphological and structural features, indicating that the deposition rate can be used as an additional parameter to tune the perovskite film properties. The device data indicate that charge transport within the film is efficient, as also supported by steady-state photocarrier grating measurements (details in the SI, Figure S7), confirming the high quality of the coevaporated MAPI films. Further studies will be directed toward the identification of the growth mechanism and the upper limit for fast deposition processes and extended to other materials such as mixed halide wide bandgap materials or narrower bandgap perovskites.

■ ASSOCIATED CONTENT

Supporting Information

The Supporting Information is available free of charge at https://pubs.acs.org/doi/10.1021/acsenergylett.3c01724.

Materials, device fabrication and characterization, process parameters, optical absorption, AFM, additional opto-electronic characterization, and steady-state photocarrier grating (PDF)

■ AUTHOR INFORMATION

Corresponding Authors

Michele Sessolo − *Instituto de Ciencia Molecular, Universidad de Valencia, 46980 Paterna, Spain;* orcid.org/0000-0002-9189-3005; Email: michele.sessolo@uv.es

Henk Bolink − *Instituto de Ciencia Molecular, Universidad de Valencia, 46980 Paterna, Spain;* orcid.org/0000-0001-9784-6253; Email: henk.bolink@uv.es

Authors

Manuel Piot − *Instituto de Ciencia Molecular, Universidad de Valencia, 46980 Paterna, Spain*

Javier Enrique Sebastian Alonso − *Instituto de Ciencia Molecular, Universidad de Valencia, 46980 Paterna, Spain*

Kassio P. S. Zanoni − *Instituto de Ciencia Molecular, Universidad de Valencia, 46980 Paterna, Spain;* orcid.org/0000-0003-4586-6126

Nathan Rodkey − *Instituto de Ciencia Molecular, Universidad de Valencia, 46980 Paterna, Spain*

Federico Ventosinos − *Instituto de Ciencia Molecular, Universidad de Valencia, 46980 Paterna, Spain*

Cristina Roldán-Carmona − *Instituto de Ciencia Molecular, Universidad de Valencia, 46980 Paterna, Spain*

Complete contact information is available at: https://pubs.acs.org/10.1021/acsenergylett.3c01724

Notes

The authors declare no competing financial interest.

■ ACKNOWLEDGMENTS

The authors acknowledge financial support of the European Research Council (ERC) under the European Union's Horizon 2020 research and innovation programme (Grant Agreement No. 834431). Authors acknowledge support from the Comunitat Valenciana (projects CISEJI/2022/43 and IDIFEDER/2021/078), as well as from the Ministry of Science and Innovation (MCIN) and the Spanish State Research Agency (AEI): project TED2021-129679B-C21 and grant IJC2020-045130-I funded by MCIN/AEI/10.13039/501100011033 and by the "European Union NextGenerationEU/PRTR"; María Zambrano fellowship ZA21-064; grant RYC2019-027187-I funded by MCIN/AEI/10.13039/501100011033 and by "ESF Investing in Your Future"; project CEX2019-000919-M funded by MCIN/AEI/10.13039/501100011033.

■ REFERENCES

(1) Lee, J.; et al. Opportunities and Challenges for Perovskite Solar Cells Based on Vacuum Thermal Evaporation. *Adv. Mater. Technol.* **2022**, 2200928.

(2) Chin, X. Y.; et al. Interface Passivation for 31.25%-Efficient Perovskite/Silicon Tandem Solar Cells. *Science (80-.)* **2023**, *381* (6653), 59−63.

(3) Momblona, C.; et al. Efficient Vacuum Deposited P-i-n and n-i-p Perovskite Solar Cells Employing Doped Charge Transport Layers. *Energy Environ. Sci.* **2016**, *9* (11), 3456−3463.

(4) Li, J.; et al. Highly Efficient Thermally Co-Evaporated Perovskite Solar Cells and Mini-Modules. *Joule* **2020**, *4* (5), 1035−1053.

(5) Roß, M.; et al. Co-Evaporated p-i-n Perovskite Solar Cells beyond 20% Efficiency: Impact of Substrate Temperature and Hole-Transport Layer. *ACS Appl. Mater. Interfaces* **2020**, *12* (35), 39261−39272.

(6) Roß, M.; et al. Co-Evaporated Formamidinium Lead Iodide Based Perovskites with 1000 h Constant Stability for Fully Textured Monolithic Perovskite/Silicon Tandem Solar Cells. *Adv. Energy Mater.* **2021**, *11* (35), 2101460.

(7) Feng, J.; et al. High-Throughput Large-Area Vacuum Deposition for High-Performance Formamidine-Based Perovskite Solar Cells. *Energy Environ. Sci.* **2021**, *14* (5), 3035−3043.

(8) Li, H.; et al. Sequential Vacuum-Evaporated Perovskite Solar Cells with More than 24% Efficiency. *Sci. Adv.* **2022**, *8* (28), eabo7422 DOI: 10.1126/sciadv.abo7422.

(9) Kim, B.-S.; et al. Deposition Kinetics and Compositional Control of Vacuum-Processed CH 3 NH 3 PbI 3 Perovskite. *J. Phys. Chem. Lett.* **2020**, *11* (16), 6852−6859.

(10) Lohmann, K. B.; et al. Control over Crystal Size in Vapor Deposited Metal-Halide Perovskite Films. *ACS Energy Lett.* **2020**, *5* (3), 710−717.

(11) Zanoni, K. P. S.; et al. Photovoltaic Devices Using Sublimed Methylammonium Lead Iodide Perovskites: Long-Term Reproducible Processing. *Sol. RRL* **2023**, *7* (7), 2201073 DOI: 10.1002/solr.202201073.

(12) Palazon, F.; et al. Room-Temperature Cubic Phase Crystallization and High Stability of Vacuum-Deposited Methylammonium Lead Triiodide Thin Films for High-Efficiency Solar Cells. *Adv. Mater.* **2019**, *31* (39), 1902692.

(13) Ávila, J.; et al. Vapor-Deposited Perovskites: The Route to High-Performance Solar Cell Production? *Joule* **2017**, *1* (3), 431−442.